Original Research *Highlight article*

Boronate probe-based hydrogen peroxide detection with AlGaN/GaN HEMT sensor

Isra Mahaboob, Roger J Reinertsen, Benjamin McEwen, Kasey Hogan, Emma Rocco, J Andres Melendez, Nathaniel C Cady and F Shahedipour-Sandvik

College of Nanoscale Science and Engineering, SUNY Polytechnic Institute, Albany, NY 12203, USA
Corresponding author: Isra Mahaboob. Email: imahaboob@sunypoly.edu

Impact statement

This study presents a novel application of a surface sensitive electronic sensor made up of a biocompatible semiconducting material system (Al)GaN, for the detection of reactive oxygen species present in biological settings that contain hydrogen peroxide. The results from this study demonstrate the possibilities of interfacing biocompatible electronics with existing bioorthogonal probes to expand the capabilities of existing detection techniques. Additionally, this opens new avenues for the development of future hybrid electro-chemical sensing systems which can interface with living systems and allow real-time remote monitoring.

Abstract

The results from this study demonstrate the potential of an AlGaN/GaN high electron mobility transistor sensor for the detection of reactive and transient biological molecules such as hydrogen peroxide. A boronate-based fluorescent probe was used with this device to detect the presence of micromolar levels of hydrogen peroxide typically associated with intracellular processes. The real-time electrical response of the high electron mobility transistor sensor showed a gradual decrease in the two-dimensional electron gas current as the reaction proceeded over time. A corresponding increase in the emission intensity was measured from the fluorescent probe with the progression of the reaction. The fluorescence from the boronate probe was used as an indicator to confirm the detection of hydrogen peroxide. These results demonstrate the dynamic measurement capability of AlGaN/GaN high electron mobility transistor sensors in monitoring real-time reactions of reactive oxygen species such as hydrogen peroxide.

Keywords: Hydrogen peroxide, AlGaN/GaN HEMT, ROS, HEMT sensors, boronate probe, electrochemical sensing

Experimental Biology and Medicine **2021; 246: 523–528. DOI: 10.1177/1535370220972030**

Introduction

Over the last three decades, a tremendous amount of research has been conducted in the development of the III-nitride (III-N) material system and device technology.[1–13] III-N-based AlGaN/GaN high electron mobility transistors (HEMTs) have been extensively studied for biochemical sensing applications due to their high sensitivity to surface phenomena, fast response time, aqueous stability, and good biocompatibility.[14–17] In HEMT sensors, the two-dimensional electron gas (2DEG) acts as a highly conductive channel that can be modulated by changes in the surface potential. The detected signal in the gate region is amplified and measured as a change in the 2DEG conductivity, which makes the HEMT a good sensing device. Based on this principle, HEMT sensors have demonstrated promising results in the detection of pH changes,[18,19] gas molecules,[20–22] DNA,[23,24] and cancer-associated antigens,[25,26] as well as in monitoring living cells.[27,28] Due to their unique electrical and chemical properties, the AlGaN/GaN HEMTs show great potential for the detection of reactive and transient biological components, such as reactive oxygen species (ROS). Amongst the various ROS molecules, hydrogen peroxide (H_2O_2) is widely studied, as it is relatively stable and abundant in comparison to other ROS molecules. H_2O_2 also has been implicated in various roles, both beneficial and detrimental to cellular health.[29–31] As a beneficial species, it is used as a signaling molecule to regulate various cellular processes. On the other hand, high levels of H_2O_2 have been shown to cause oxidative stress, which is associated with damage to cellular structures, aging, neuro-degenerative diseases, and the formation of malignant cells. To understand the complex roles played by H_2O_2, several techniques have been developed to detect and monitor it in its native settings with high selectivity and sensitivity.[32–35] One of the conventional approaches for detection involves the use of fluorescent probes which react specifically with H_2O_2.[36,37] Though such a method is reliable, it is time-consuming and involves extensive processing. To overcome limitations of the conventional approaches while utilizing their

advantages, there is a strong interest in the development of hybrid electro-chemical sensing systems, as detection based on electron transport can generate larger and faster signals.[28] Additionally, electro-chemical detection offers the potential advantage of real-time and remote monitoring through the development of integrated sensing platforms. In this letter, we report the use of an AlGaN/GaN HEMT-based sensor for detection of the presence of H_2O_2 by correlating its measured change in conductivity with a reaction of H_2O_2 and a boronate-based fluorescent probe in the gate-well region. Here, we utilize the high selectivity of the boronate probe to detect H_2O_2, and the surface sensitivity of HEMTs to generate a corresponding electrical response. A non-functionalized, non-metallized open-gate AlGaN/GaN HEMT sensor is employed in this study. The real-time progression of the reaction is monitored by measuring the modulation of the 2DEG current in response to changes in the surface potential caused by the interaction between the semiconductor surface states and the products of the reaction. The response of our HEMT sensor shows its applicability to the detection of micro-molar concentrations of H_2O_2, which is in the range typically present in intracellular processes of living systems.[29,31,36,38]

Materials and methods

The AlGaN/GaN HEMT sensor employed in this study was fabricated on a HEMT structure consisting of a ~4 μm thick nominally undoped GaN buffer layer, 20 nm thick $Al_{0.3}Ga_{0.7}N$ barrier layer, and 4 nm thick Si-doped n^+GaN cap layer. The epilayers were grown by metal organic chemical vapor deposition on a 2-inch sapphire substrate.[39–41] Hall effect measurement on this structure showed a 2DEG density of 1.43×10^{13} cm^{-2}, carrier mobility of 1060 cm^2/V-s, and sheet resistance of 418 Ω/sq. Mesas roughly 250 nm in height were formed by inductively coupled plasma etching using low power $BCl_3/Cl_2/Ar$ chemistry to isolate active device area from rest of the substrate. Source and drain ohmic contacts consisting of Ti (15 nm)/Al (60 nm)/Mo (35 nm)/Au (80 nm) multilayer stacks were deposited and annealed at 850°C in nitrogen ambient for 30 s. SU-8 negative photoresist was used to encapsulate the source/drain contacts and to create a well-type region in the gate area for liquid testing. The dimension of the gate-well region was 100 μm × 140 μm. An optical image of the fabricated device is shown in Figure 1. Electrical conductivity between the source and drain terminals was measured at room temperature using an Agilent B1500A semiconductor device parameter analyzer.

The boronate-based fluorescent probe Peroxy Orange 1 (PO1) was employed for the detection of H_2O_2.[34,36] Boronate probes are bioorthogonal and well-established for the detection and imaging of H_2O_2 in biological settings with high selectivity and sensitivity.[34] Selectivity tests have shown negligible turn-on of boronate probes in the presence of other ROS molecules. These probes undergo an irreversible reaction into a fluorescent state upon reaction with H_2O_2, which is advantageous in detecting transient and low levels of H_2O_2 in living systems. From previous reports, the boronate probes can reliably detect H_2O_2 concentrations as low as tens of micromolar to hundreds of nanomolar in aqueous solution.[42] While the presence of an optical transition is required for the fluorometric usage of these probes, it is not required for electrical detection where factors such as charge, and adsorption behavior are more important. In this study, the charge associated with the reaction products is utilized to generate a corresponding electrical response. Additionally, the ability to measure reaction progress through fluorescence allows for the comparison of optical and electrical detection of

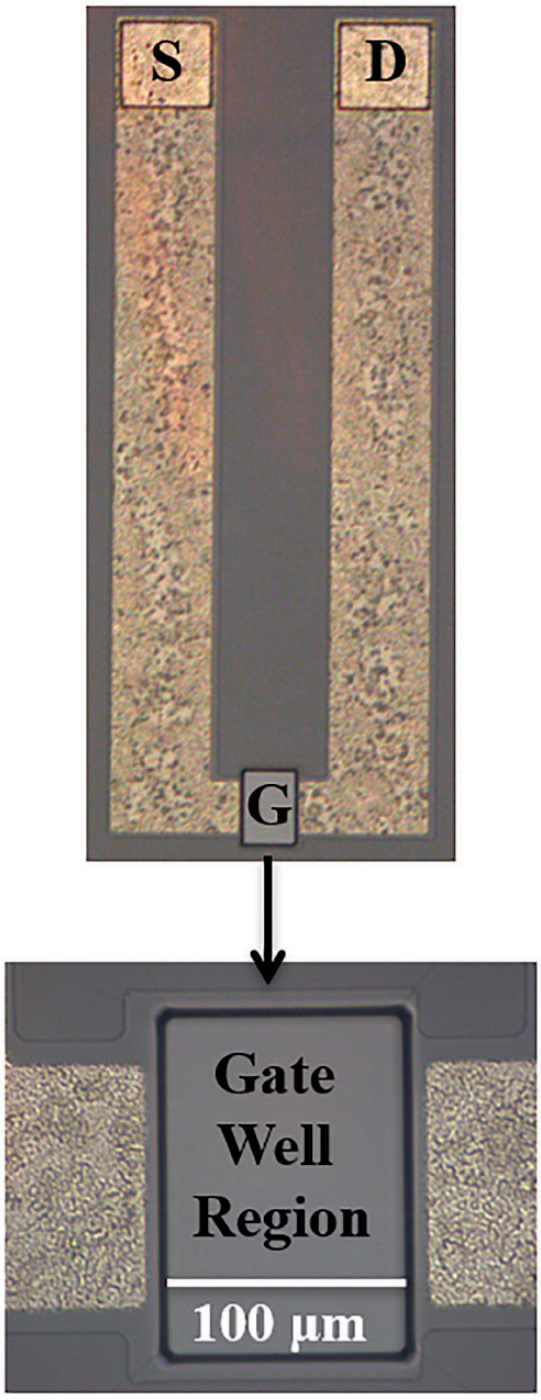

Figure 1. Optical image of fabricated AlGaN/GaN HEMT sensor. (A color version of this figure is available in the online journal.)

the reaction. The reagents, H_2O_2 and PO1, were obtained from Sigma Aldrich. Dilutions of H_2O_2 were prepared on the days of testing by diluting a stock (35% by weight) in deionized water to obtain fresh solutions containing micromolar concentrations of H_2O_2. In this study, anhydrous dimethyl sulfoxide (DMSO) was used as a solvent to prepare solutions of the boronate probe PO1, as it is a known standard for this type of reagent.[36] Previous reports indicate that DMSO shows almost negligible reactivity with H_2O_2 under the current test conditions.[43,44] During testing, appropriate volumes of this solution were added to dilute aqueous H_2O_2 to obtain a probe concentration of 5 μM in the final solution, as per the manufacturer instructions.

Electrical measurements were performed after transferring the test solution into the gate-well region of the device via a microfluidic line. Source-to-drain channel current (I_{DS}) measurements were conducted to investigate how the 2DEG conductivity changed as a function of time. A low drain-source voltage ($V_{DS} = 100$ mV) was utilized to prevent any electrochemical reactions and to minimize the heat generation in the device associated with high current densities. Measurements were performed in a dark environment at room temperature. Initial electrical measurements with aqueous H_2O_2 solutions of varying concentration confirmed that the 2DEG current does not change with the addition of dilute peroxide alone. This is expected, because the detection mechanism of an AlGaN/GaN HEMT sensor depends on the electrostatic interaction between the analytes and electronic surface states of the device. As such, neutrally charged molecules such as H_2O_2 are not expected to generate a strong response. Molecules with specific reactivity towards H_2O_2 such as the boronate probes which are used in this study, generate charged products upon reaction with H_2O_2 which enables indirect detection. Baseline measurements were first performed by testing DMSO+PO1+H_2O solutions not containing any H_2O_2. Subsequent measurements were performed after adding the DMSO+PO1 mixture to the H_2O_2 dilutions. To ensure homogeneous composition, the solutions were mixed well before transfer onto the gate-well region. Once the reaction was started, the real-time response of HEMTs was monitored for 200 s intervals at different points in the reaction.

Results

The electrical response of the HEMT sensor to test solutions initially containing 25 μM and 12.5 μM concentration of H_2O_2 with 5 μM boronate probe solution deposited in the gate-well region is shown in Figure 2(a) and (b),

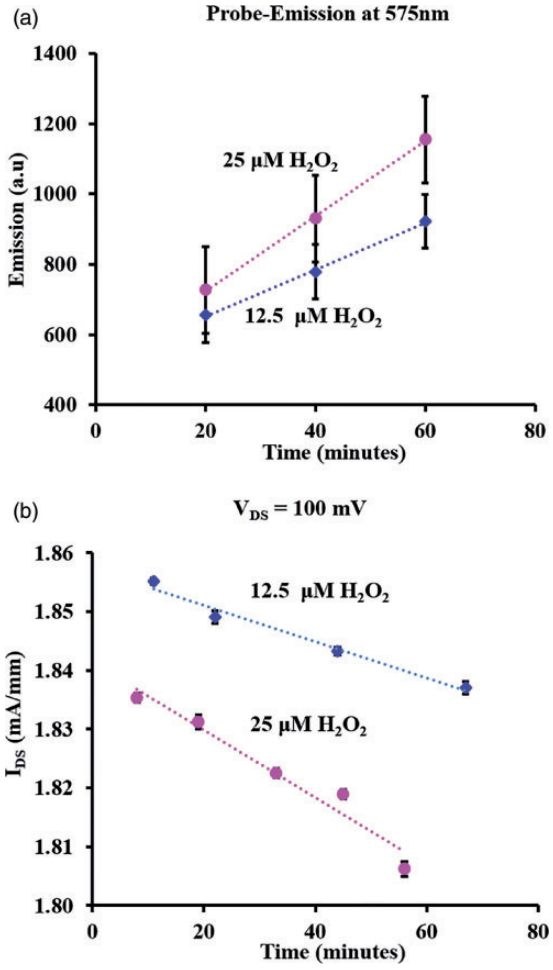

Figure 3. (a) Fluorescence emission over time, and (b) electrical measurements showing real-time change in 2DEG current for H_2O_2 solutions of 25 μM (magenta trend line with circular markers) and 12.5 μM (blue trend line with diamond markers). The dashed lines between points are a guide for the eye. (A color version of this figure is available in the online journal.)

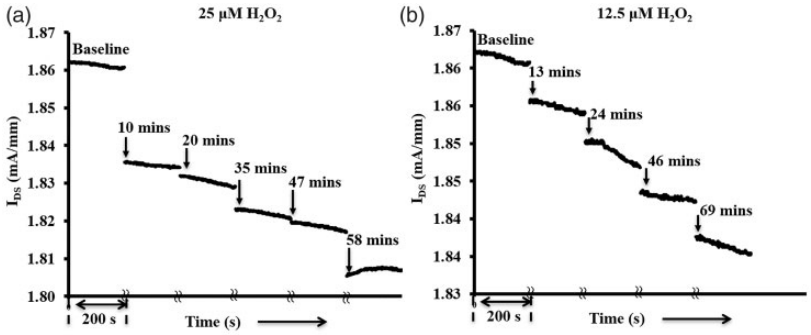

Figure 2. 2DEG channel current measurement as a function of time at $V_{DS} = 100$ mV with (a) 25 μM and (b) 12.5 μM of H_2O_2. The real-time response of the device was tested for 200 s, first with baseline solution (DMSO + PO1+ H_2O), and then at different reaction times after the addition of H_2O_2 to the baseline solution.

respectively. From the figure, for a fixed concentration of the boronate probe (5 μM), a higher rate of decrease in 2DEG current is observed in the test with the higher concentration of H_2O_2. A decrease in the 2DEG current by 0.029 mA/mm and 0.018 mA/mm was measured after the reaction had proceeded for about an hour with solutions initially containing 25 μM and 12.5 μM of H_2O_2, respectively.

To confirm the expected reaction between PO1 and H_2O_2, as well as to characterize the rate of the reaction, the fluorescent emission of the reaction mixture was measured at various intervals as the reaction progressed with a FlexStation-3 fluorescence plate reader from Molecular Devices. Maximum emission of the probe was measured at 575 nm wavelength with an excitation wavelength of 540 nm. Figure 3(a) shows the intensity of the emission from the activated fluorescent probes generated upon reaction with H_2O_2, measured by the fluorescence plate reader. The intensity of the emission increases with the concentration of H_2O_2, which is in agreement with previous reports.[37] Comparing the trends from the optical (Figure 3(a)) and the electrical measurements (Figure 3(b)), it can be seen that as the reaction proceeds, an increase in the emission intensity and a corresponding decrease in 2DEG current is observed. For a fixed probe concentration, emission intensity is higher for solutions with higher initial concentration of H_2O_2, which corresponds with a larger decrease in the 2DEG current.

Discussion

The sensing mechanism of the HEMT device involves detection of the changes in the surface potential correlated with the reaction between H_2O_2 and the boronate probe. From the electrical characterization data, a steady decrease in the 2DEG channel current was measured over time as the reaction proceeds. It is well known that changes in the charge accumulated at the liquid/semiconductor interface directly affect the surface states of the semiconductor. Due to this, the electrostatic compensation which exists between the surface states and 2DEG is misbalanced, which results in modulation of the 2DEG current.[45–47] The reaction between the boronate probe and H_2O_2 molecules results in the release of an activated fluorescent probe and a weakly acidic pinacol boronic acid, as can be seen in Figure 4. The real-time electrical response of the 2DEG current, shown in Figure 2, indicates accumulation of net negative surface charge at the liquid/semiconductor interface as the reaction progresses. The accumulation of negative surface charge is attributed to the interaction of the delocalized Π electrons and charged carboxylate group in the activated boronate probe with the surface states of HEMT. As more products are generated, a gradual decrease in the 2DEG current is observed over time, as illustrated in Figure 4(b). Comparing the rate of change in the emission and electrical response shown in Figure 3, increasing the initial concentration of H_2O_2 from 12.5 μM to 25 μM amplifies the rate of increase in the emission by a factor of 1.6 and the rate of decrease in the 2DEG conductivity by a factor of 1.9, which suggests higher sensitivity of the electrical response to H_2O_2 detection in this range. These trends further demonstrate the ability of HEMT sensors in detecting H_2O_2 at concentration levels typically associated with intracellular processes. Additional work focused on functionalization of the gate region will enhance the selectivity of the

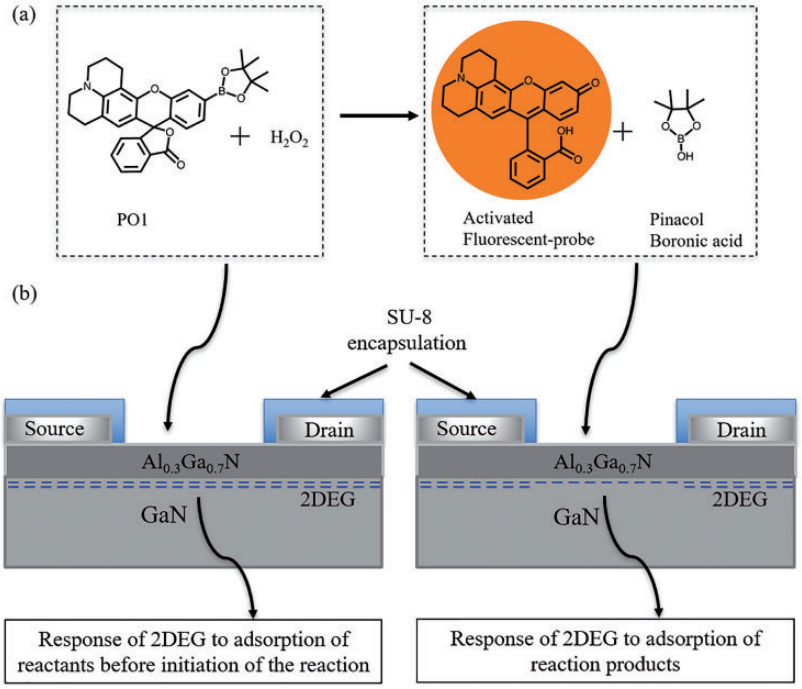

Figure 4. (a) Illustration of the reaction between boronate probe PO1 and H_2O_2 (Adapted from Lippert *et al*.[34] and Lin *et al*.[36]). The reaction results in the release of an activated fluorescent probe and a weakly acidic pinacol boronic acid. (b) Schematic representation of 2DEG modulation to the adsorption of reactants (left) and reaction products (right) to the HEMT surface. (A color version of this figure is available in the online journal.)

sensor in biological settings in the presence of other charged molecules, enabling *in vitro* utilization.

Conclusions

An AlGaN/GaN HEMT sensor was used in the present work to detect H_2O_2 using a boronate-based fluorescent probe. The sensitivity of the HEMT surface to changes in the surface potential was utilized to successfully measure the progress of the reaction between a boronate-probe and H_2O_2. Observations from this study confirm the dynamic sensing capability of HEMT sensors in monitoring real-time changes which occur during the reaction between a ROS molecule, such as H_2O_2, and a molecule with specific reactivity. The biocompatible and stable nature of the III-N material system opens new possibilities for the development of AlGaN/GaN HEMT sensors which can interface with living cells to understand the complex functionality of ROS molecules in their native settings.

AUTHORS' CONTRIBUTIONS

IM and RJR performed experiments, measurements, data collection, analysis, visualization, and writing of the article; BM participated in formal analysis, discussion, and review of the article; KH and ER contributed towards maintenance and support with semiconductor material growth; JAM, NCC and FSS were involved in supervision, methodology, resources, validation, and review of the article.

ACKNOWLEDGEMENTS

IM and RJR greatly acknowledge the valuable insights provided by Dr. Nathan Lazarus and Dr. Radislav Potyrailo.

DECLARATION OF CONFLICTING INTERESTS

The author(s) disclosed receipt of the following financial support for the research, authorship, and/or publication of this article: The author(s) declare no potential conflicts of interest with respect to the research, authorship, and/or publication of this article.

FUNDING

This work was supported in part by Army Research Laboratory [Grant # W911NF-16–2-0031].

ORCID IDS

Isra Mahaboob https://orcid.org/0000-0001-7155-8130
J Andres Melendez https://orcid.org/0000-0001-8021-3097
Nathaniel C Cady https://orcid.org/0000-0003-4345-3627

REFERENCES

1. Bulmer J, Suvarna P, Leathersich J, Marini J, Mahaboob I, Newman N, Shahedipour-Sandvik F. Visible-blind APD heterostructure design with superior field confinement and low operating voltage. *IEEE Photon Technol Lett* 2016;**28**:39–42
2. Mahaboob I, Yakimov M, Hogan K, Rocco E, Tozier S, Shahedipour-Sandvik F. Dynamic control of AlGaN/GaN HEMT characteristics by implementation of a p-GaN body-diode-based back-gate. *IEEE J Electron Devices Soc* 2019;**7**:581–8
3. Mahaboob I, Yakimov M, Rocco E, Hogan K, Shahedipour-Sandvik F. Drain-Voltage-Induced secondary effects in AlGaN/GaN HEMTs with integrated Body-Diode. *IEEE Trans Electron Devices* 2020;**67**:3983–7
4. Marini J, Mahaboob I, Rocco E, Bell LD, Shahedipour-Sandvik F. Polarization engineered N-polar Cs-free GaN photocathodes. *J Appl Phys* 2018;**124**:113101
5. Suvarna P, Bulmer J, Leathersich JM, Marini J, Mahaboob I, Hennessy J, Bell LD, Nikzad S, Shahedipour-Sandvik F. Ion Implantation-Based edge termination to improve III-N APD reliability and performance. *IEEE Photon Technol Lett* 2015;**27**:498–501
6. Marini J, Mahaboob I, Hogan K, Novak S, Bell LD, Shahedipour-Sandvik F. Mg incorporation efficiency in pulsed MOCVD of N-Polar GaN:Mg. *J Elec Mater* 2017;**46**:5820–6
7. Marini J, Leathersich J, Mahaboob I, Bulmer J, Newman N, Shahedipour-Sandvik F. MOCVD growth of N-polar GaN on on-axis sapphire substrate: impact of AlN nucleation layer on GaN surface hillock density. *J Cryst Growth* 2016;**442**:25–30
8. Rocco E, Licata O, Mahaboob I, Hogan K, Tozier S, Meyers V, McEwen B, Novak S, Mazumder B, Reshchikov M, Bell LD, Shahedipour-Sandvik F. Hillock assisted p-type enhancement in N-polar GaN:Mg films grown by MOCVD. *Sci Rep* 2020;**10**:1426
9. Meyers V, Rocco E, Hogan K, Tozier S, McEwen B, Mahaboob I, Shahedipour-Sandvik F. Removal of dry-etch-induced surface layer damage from p-GaN by photoelectrochemical etching. *J Elec Mater* 2020;**49**:3481–9
10. Tompkins RP, Mahaboob I, Shahedipour-Sandvik F, Lazarus N. Mechanical analysis of stretchable AlGaN/GaN high electron mobility transistors. *ECS Transac* 2016;**72**:89–95
11. Hogan K, Tozier S, Rocco E, Mahaboob I, Meyers V, McEwen B, Shahedipour-Sandvik F, Tompkins R, Derenge M, Jones K, Shevelev M, Sklyar V, Lang A, Hart J, Taheri M and Reshchikov M. Novel gyrotron beam annealing method for Mg-implanted bulk GaN. *IEEE Int Reliab Phys Symp* 2019;1–6. doi: 10.1109/IRPS.2019.8720600
12. Nikzad S, Hoenk M, Jewell AD, Hennessy JJ, Carver AG, Jones TJ, Goodsall TM, Hamden ET, Suvarna P, Bulmer J, Shahedipour-Sandvik F, Charbon E, Padmanabhan P, Hancock B, Douglas Bell L. Single photon counting UV solar-blind detectors using silicon and III-Nitride materials. *Sensors* 2016;**6**:927
13. Mahaboob I, Novak SW, Rocco E, Hogan K, Shahedipour-Sandvik F. Investigation of the electrical behavior of AlGaN/GaN high electron mobility transistors grown with underlying GaN:Mg layer. *J Vac Sci Technol B* 2018;**36**:031203
14. Ren F, Pearton SJ. Sensors using AlGaN/GaN based high electron mobility transistor for environmental and bio-applications. *ECS Trans* 2013;**53**:1–17
15. Pearton SJ, Ren F, Wang Y-L, Chu BH, Chen KH, Chang CY, Lim W, Lin J, Norton DP. Recent advances in wide bandgap semiconductor biological and gas sensors. *Prog Mater Sci* 2010;**55**:1–59
16. Chaniotakis N, Sofikiti N. Novel semiconductor materials for the development of chemical sensors and biosensors: a review. *Anal Chim Acta* 2008;**615**:1–9
17. Stutzmann M, Steinhoff G, Eickhoff M, Ambacher O, Nebel CE, Schalwig J, Neuberger R, Muller G. GaN-based heterostructures for sensor applications. *Diam Relat Mater* 2002;**11**:886–91
18. Steinhoff G, Hermann M, Schaff WJ, Eastman LF, Stutzmann M, Eickhoff M. pH response of GaN surfaces and its application for pH-sensitive field-effect transistors. *Appl Phys Lett* 2003;**83**:177
19. Abidin MSZ, Hashim AM, Sharifabad ME, Abd Rahman SF, Sadoh T. Open-gated pH sensor fabricated on an undoped-AlGaN/GaN HEMT structure. *Sensors* 2011;**11**:3067–77
20. Ali M, Cimalla V, Lebedev V, Romanus H, Tilak V, Merfeld D, Sandvik P, Ambacher O. Pt/GaN schottky diodes for hydrogen gas sensors. *Sensors Actuators B Chem* 2006;**113**:797–804
21. Pearton SJ, Ren F. Gallium Nitride-Based gas, chemical and biomedical sensors. *IEEE Instrum Meas Mag* 2012;**15**:16–21

22. Lim M, Mills S, Lee B, Misra V. Application of AlGaN/GaN heterostructures for ultra-low power nitrogen dioxide sensing. *ECS J Solid State Sci Technol* 2015;**4**:S3034–S3037
23. Xu X, Jindal V, Shahedipour-Sandvik F, Bergkvist M, Cady NC. Direct immobilization and hybridization of DNA on group III nitride semiconductors. *Appl Surf Sci* 2009;**255**:5905–9
24. Fahrenkopf NM, Shahedipour-Sandvik F, Tokranova N, Bergkvist M, Cady NC. Direct attachment of DNA to semiconducting surfaces for biosensor applications. *J Biotechnol* 2010;**150**:312–4
25. Chen KH, Kang BS, Wang HT, Lele TP, Ren F, Wang YL, Chang CY, Pearton SJ, Dennis DM, Johnson JW, Rajagopal P, Roberts JC, Piner EL, Linthicum KJ. c-erbB-2 sensing using AlGaN/GaN high electron mobility transistors for breast cancer detection. *Appl Phys Lett* 2008;**92**:192103
26. Kang BS, Wang HT, Lele TP, Tseng Y, Ren F, Pearton SJ, Johnson JW, Rajagopal P, Roberts JC, Piner EL, Linthicum KJ. Prostate specific antigen detection using AlGaN/GaN high electron mobility transistors. *Appl Phys Lett* 2007;**91**:112106
27. Young T-H, Chen C-R. Assessment of GaN chips for culturing cerebellar granule neurons. *Biomaterials* 2006;**27**:3361–7
28. Kirste R, Rohrbaugh N, Bryan I, Bryan Z, Collazo R, Ivanisevic A. Electronic biosensors based on III-Nitride semiconductors. *Annu Rev Anal Chem* 2015;**8**:149–69
29. Breton-Romero R, Lamas S. Hydrogen peroxide signaling in vascular endothelial cells. *Redox Biol* 2014;**2**:529–34
30. Veal EA, Day AM, Morgan BA. Hydrogen peroxide sensing and signaling. *Mol Cell* 2007;**26**:1–14
31. Marinho HS, Real C, Cyrne L, Soares H, Antunes F. Hydrogen peroxide sensing, signaling and regulation of transcription factors. *Redox Biol* 2014;**2**:535–62
32. Palanisamy S, Cheemalapati S, Chen SM. Highly sensitive and selective hydrogen peroxide biosensor based on hemoglobin immobilized at multiwalled carbon nanotubes-zinc oxide composite electrode. *Anal Biochem* 2012;**429**:108–15
33. Chen W, Cai S, Ren Q, Wen W, Zhao Y. Recent advances in electrochemical sensing for hydrogen peroxide: a review. *Analyst* 2012;**137**:49–58
34. Lippert AR, Van De Bittner GC, Chang CJ. Boronate oxidation as a bioorthogonal reaction approach for studying the chemistry of hydrogen peroxide in living systems. *Acc Chem Res* 2011;**44**:793–804
35. Sun X, Xu S-Y, Flower SE, Fossey JS, Qian X, James TD. Integrated' and 'insulated' boronate-based fluorescent probes for the detection of hydrogen peroxide. *Chem Commun* 2013;**49**:8311–3
36. Lin VS, Dickinson BC, Chang CJ. Boronate-based fluorescent probes: imaging hydrogen peroxide in living systems. *Methods Enzymol* 2013;**526**:19–43
37. Dickinson BC, Huynh C, Chang CJ. A palette of fluorescent probes with varying emission colors for imaging hydrogen peroxide signaling in living cells. *J Am Chem Soc* 2010;**132**:5906–15
38. Winterbourn CC. The challenges of using fluorescent probes to detect and quantify specific reactive oxygen species in living cells. *Biochim Biophys Acta* 2014;**1840**:730–8
39. Tompkins RP, Mahaboob I, Shahedipour-Sandvik F, Lazarus N. Electrical properties of AlGaN/GaN HEMTs in stretchable geometries. *Solid State Electron* 2017;**136**:36–42
40. Mahaboob I, Marini J, Hogan K, Rocco E, Tompkins RP, Lazarus N, Shahedipour-Sandvik F. Selective area epitaxial growth of stretchable geometry AlGaN-GaN heterostructures. *J Elec Mater* 2008;**47**:6625–34
41. Mahaboob I, Hogan K, Novak SW, Shahedipour-Sandvik F, Tompkins RP, Lazarus N. Influence of mask material on the electrical properties of selective area epitaxy GaN microstructures. *J Vac Sci Technol* 2018;**36**:031203
42. Miller EW, Albers AE, Pralle A, Isacoff EY, Chang CJ. Boronate-based fluorescent probes for imaging cellular hydrogen peroxide. *J Am Chem Soc* 2005;**127**:16652–9
43. Amels P, Elias H, Wannowius K-J. Kinetics and mechanism of the oxidation of dimethyl sulfide by hydroperoxides in aqueous medium study on the potential contribution of liquid-phase oxidation of dimethyl sulfide in the atmosphere. *Faraday Trans* 1997;**93**:2537–44
44. Ogata Y, Tanaka K. Kinetics of the oxidation of dimethyl sulfoxide with aqueous hydrogen peroxide catalyzed by sodium tungstate. *J Chem* 1981;**59**:718
45. Ibbetson JP, Fini PT, Ness KD, DenBaars SP, Speck JS, Mishra UK. Polarization effects, surface states, and the source of electrons in AlGaN/GaN heterostructure field effect transistors. *Appl Phys Lett* 2000;**77**:250
46. Koley G, Spencer MG. On the origin of the two-dimensional electron gas at the AlGaN/GaN heterostructure interface. *Appl Phys Lett* 2005;**86**:042107
47. Ambacher O, Smart J, Shealy JR, Weimann NG, Chu K, Murphy M, Schaff WJ, Eastman LF, Dimitrov R, Wittmer L, Stutzmann M, Rieger W, Hilsenbeck J. Two-dimensional electron gases induced by spontaneous and piezoelectric polarization charges in N- and Ga-face AlGaN/GaN heterostructures. *J. Appl. Phys* 1999;**85**:3222

(Received September 9, 2020, Accepted October 15, 2020)